



HAL
open science

Controlled *E. coli* aggregation mediated by DNA and XNA hybridization. Authors

Cécile Gasse, Puneet Srivastava, Guy Shepers, Joachim Jose, Marcel Hollenstein, Philippe Marlière, Piet Herdewijn

► To cite this version:

Cécile Gasse, Puneet Srivastava, Guy Shepers, Joachim Jose, Marcel Hollenstein, et al.. Controlled *E. coli* aggregation mediated by DNA and XNA hybridization. Authors. *ChemBioChem*, In press, pp.e202300191. 10.1002/cbic.202300191 . pasteur-04104867

HAL Id: pasteur-04104867

<https://pasteur.hal.science/pasteur-04104867>

Submitted on 24 May 2023

HAL is a multi-disciplinary open access archive for the deposit and dissemination of scientific research documents, whether they are published or not. The documents may come from teaching and research institutions in France or abroad, or from public or private research centers.

L'archive ouverte pluridisciplinaire **HAL**, est destinée au dépôt et à la diffusion de documents scientifiques de niveau recherche, publiés ou non, émanant des établissements d'enseignement et de recherche français ou étrangers, des laboratoires publics ou privés.



Distributed under a Creative Commons Attribution - NonCommercial 4.0 International License

Title:

Controlled *E. coli* aggregation mediated by DNA and XNA hybridization.

Authors:

Cécile Gasse*, Puneet Srivastava, Guy Schepers, Joachim Jose, Marcel Hollenstein, Philippe Marlière, Piet Herdewijn*

Summary

Chemical cell surface modification is a fast-growing field of research, due to its enormous potential in tissue engineering, cell-based immunotherapy, and regenerative medicine. However, engineering of bacterial tissues by chemical cell surface modification has been vastly underexplored and the identification of suitable molecular handles is in dire need. We present here, an orthogonal nucleic acid-protein conjugation strategy to promote artificial bacterial aggregation. This system gathers the high selectivity and stability of linkage to a protein Tag expressed at the cell surface and the modularity and reversibility of aggregation due to oligonucleotide hybridization. For the first time, XNA (xeno nucleic acids in the form of 1,5-anhydrohexitol nucleic acids) were immobilized *via* covalent, SNAP-tag-mediated interactions on cell surfaces to induce bacterial aggregation.

[*] Dr. Cécile Gasse

Génomique Métabolique, Genoscope, Institut François Jacob, CEA, CNRS, Univ Evry, Université Paris-Saclay, 2 Rue Gaston Crémieux, 91057 Evry, France
E-mail: cecile.gasse@univ-evry.fr

[*] Prof. Piet Herdewijn, Dr. Puneet Srivastava, Guy Schepers

Laboratory of Medicinal Chemistry, Rega Institute for Biomedical Research, KU Leuven, Herestraat 49, Box 1041, 3000 Leuven, Belgium
E-mail: piet.herdewijn@kuleuven.be

Dr. P. Marlière

The European Syndicate of Synthetic Scientists and Industrialists (TESSSI) 81 rue Réaumur, 75002 Paris (France)

Dr. Marcel Hollenstein

Institut Pasteur, Université Paris Cité, Department of Structural Biology and Chemistry, Laboratory for Bioorganic Chemistry of Nucleic Acids, CNRS UMR3523, 28, rue du Docteur Roux, 75724 Paris Cedex 15, France

Prof. Joachim Jose

Institute of Pharmaceutical and Medicinal Chemistry, University of Münster, Münster, Germany

INTRODUCTION

Engineering of cell surfaces is a rapidly developing research area because of its applicability to many practical applications including tissue engineering,¹⁻⁴ stem cells differentiation or homing,^{5,6} modulation of cell-cell signaling pathways,⁷ immuno- and/or cancer therapies.⁸⁻¹² Studies to induce reversible cell assembly of red blood cells have been triggered by clinical interest,¹³ and have led to a steady increase in the development of potent tools for programming cell-cell interactions.¹⁴ Despite these important advances, programmed aggregation of cells applied to bacterial systems is only emerging. Manipulating bacterial aggregation by integrating artificial and modulating natural surface ligands can be harnessed in the design of alternative treatment modalities to combat antimicrobial resistance or for the construction of functional materials such as artificial biofilms.¹⁵

The boundaries of this emerging field are dictated by the selection of the chemistry used in the molecular handles integrated on cell surfaces. The criteria are rather strict since an ideal conjugation chemistry for inducing controlled, artificial cell-cell aggregations should be fully orthogonal to the biological systems so as to avoid off-target aggregations or loss of biological activity. In addition, chemical handles should not induce any undesired toxicity, and their production needs to be high yielding under *in vivo* conditions.^{15,16} In this context, Bertozzi *et al.* introduced in 2000 the Staudinger ligation reaction as biorthogonal reaction for reliable and controlled cell-cell aggregation.¹⁷ Since this pioneering work, other approaches based on covalent or non-covalent fixation have been developed for the induction of bio-orthogonal interactions between bacteria including the grafting of antigen-nanobody,^{18,19} antiparallel coiled-coil peptides,²⁰⁻²² photoswitchable proteins.^{23,24} Tagged proteins were also immobilized on bacteria cell surface for whole-cell biocatalytic purposes.²⁵⁻²⁷ Despite the recent developments, alternative, chemical and biological approaches and tools for manipulating bacterial surfaces are still in dire need.

Watson-Crick base-pairing conveys DNA a high degree of programmability which combined with its inherent robustness makes it an excellent biomaterial for the spatial control of different building blocks and their assembly into precisely defined three-dimensional nanostructures. Functionalization of the surface of mammalian cells with DNA oligonucleotides showed for instance the possibility of assembling multicellular structures,²⁸⁻³⁰ implementing a streamlined 3D paracrine signaling network,² and elucidating a mechanism of action of T cell interactions.³¹ Imaging applications have also been developed.^{32,33} But only few studies have reported the inclusion of DNA oligonucleotides on bacterial cell surfaces: lipid-DNA conjugates for selective detection of bacteria by microscopy,³⁴ aldehyde-hydrazine condensation for *S. oneidensis* attachment to coated electrode surfaces to produce electricity,^{35,36} DNA polymers to encapsulate bacteria,³⁷ DNA origami nanostructures as a vehicle to deliver antimicrobial agent,³⁸ aptamer or DNA-small molecule conjugates for cancer therapy application.^{39,40} A significant drawback of DNA engineered systems is their susceptibility to nuclease-mediated degradation. While chemical alterations of the nucleosidic scaffold can at least partially remediate this shortcoming, examples of chemically modified oligonucleotides involved in cell interactions are scarce. One of the few examples has been reported in 2021 by Gavins *et al.* where xeno nucleic acids (XNA), more specifically peptide nucleic acid (PNA), was engineered at the cell surface for fluorescence imaging applications⁴¹. More recently Lu *et al.* used a protein ligase to connect PNA to a cell surface protein.⁴²

In this article, we exploited the orthogonality and biostability of XNAs combined with SNAP-tag engineering to develop a robust and versatile methodology for mediating artificial cell-cell interactions. To do so, we genetically engineered *E. coli* to express the protein SNAP-tag at the cell surface and subsequently conjugated it to both complementary unmodified and modified oligonucleotides at the surface of two distinct cell populations forming a bacterial tissue. Interestingly, SNAP-tag technology has barely been used in bacterial systems and was mainly dedicated to the capture of environmental molecules⁴³, bioimaging⁴⁴ and bacterial cell display.⁴⁵ Covalent surface immobilization of oligonucleotides via SNAP-tag conjugation allows to induce more robust artificial contacts between non-adherent cells. The attachment of the chemically modified oligonucleotides at the cell surface is inducible, selective and covalent but the aggregation itself is non-covalent and moreover reversible. For the first time XNA and more precisely 1,5-anhydrohexitol nucleic acids (HNA) (Figure 1) were immobilized on bacterial cells using SNAP-tag as surface display system and proved to be a powerful approach for cell aggregation induction.

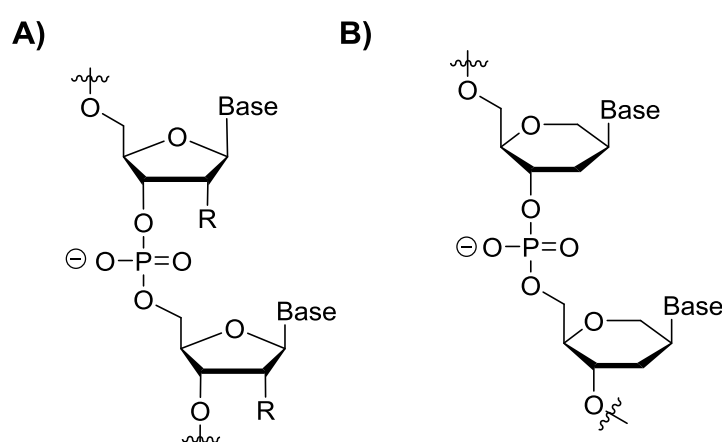


Figure 1. Chemical structures A) of canonical DNA (R = H) and RNA (R = OH) and B) of hexitol nucleic acids (HNA).

MATERIALS AND METHODS

Reagents

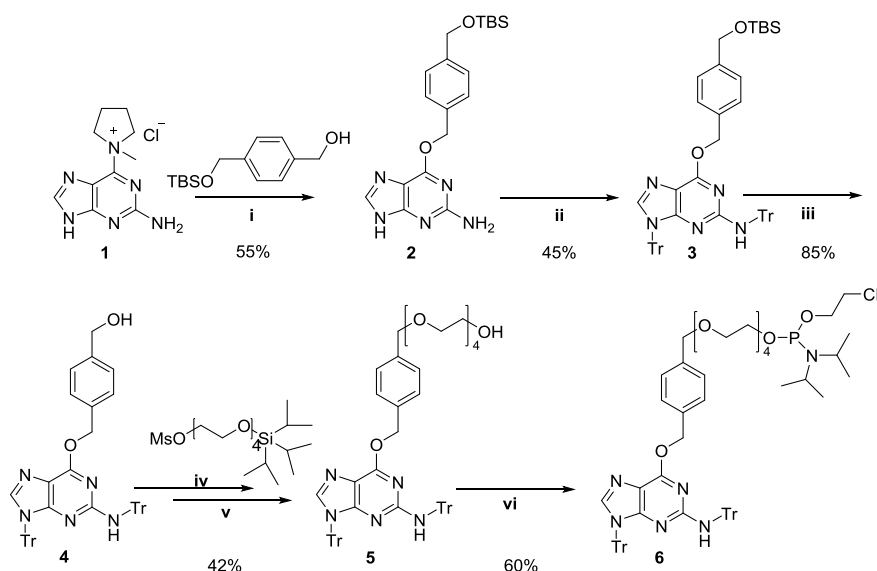
Carbenicillin disodium salt (PanReac AppliChem) and L-(+)-arabinose (Sigma-Aldrich) were supplemented to lysogeny broth (LB) medium during cell culture at a final concentration of 50 $\mu\text{g}/\text{mL}$ and 0.2 %, respectively. Propidium iodide (1.0 mg/mL solution in water, Invitrogen) and 4,6-diamidino-2-phenylindole dihydrochloride (Sigma-Aldrich, BioReagent grade) were used for fluorescence analysis at a final concentration of 1 μM and 10 $\mu\text{g}/\text{mL}$, respectively. The fluorescent label SNAP-Surface Alexa Fluor 488 was purchased from New England Biolabs, Inc. Oligonucleotides DNA₁-FAM and DNA_{1c}-TAMRA (5-regioisomer) were synthesized from Eurofins.

Synthesis of the precursor *O*⁶-Benzylguanine (BG) phosphoramidite conjugate

The synthesis of 2-cyanoethyl (1-(4-(((9-trityl-2-(tritylamino)-9*H*-purin-6-yl)oxy)methyl)phenyl)-2,5,8,11-tetraoxatridecan-13-yl)diisopropylphosphoramidite (compound **6**) started with the conjugation of mono-TBD protected 1-4 benzene dimethanol

on 1-(2-Amino-7*H*-purin-6-yl)-1-methyl-pyrrolidinium chloride followed by the protection of the guanine amine functions. Then the benzyl alcohol function was released, coupled with the linker, i.e. protected tetraethylene glycol, which was in turn finally phosphitylated (see SI part A for synthesis details).

Scheme 1



Reagents and conditions: **i.** NaH, dry DMF, 0 °C to rt, 12h; **ii.** Triphenylmethyl chloride, DMAP, DIPEA, dry DMF, 70 °C, 8-12h; **iii.** 1M TBAF, dry THF, 2h; **iv.** Potassium *tert*-butoxide, dry DMF, 0 °C to rt; **v.** 1M TBAF, dry THF, 5h. **vi.** 2-Cyanoethyl *N,N* diisopropylchlorophosphoramidite, DIPEA, CH₃CN, 4 h;

Synthesis of modified oligonucleotides

Oligonucleotides were synthesized on an Expedite DNA synthesizer (Applied Biosystems) by using the phosphoramidite approach. 3'-TAMRA CPG, 3'-(6-FAM CPG (LGC, Biosearch Technologies) and *O*⁶-Benzylguanine phosphoramidite conjugate (compound **6**) were used under standard conditions. The oligomers were cleaved from the solid support and deprotected by treatment with aqueous ammonia (30%) for 3 hours at room temperature. After gel filtration on a NAP-25 column (GE Healthcare) with water as an eluent, the crude mixture was purified on RP-HPLC (C18 column, Kinetex) using a gradient of NaClO₄ in 15% CH₃CN and 20 mM Tris-HCl buffer, pH 7.4 at the flow rate of 1 mL·min⁻¹. Oligomers were characterized by mass spectrometry (see Supporting Information).

Bacterial strain, growth conditions and cells preparation before treatment

E. coli UT5600 (F⁻, araC14, leuB6(Am), secA206(aziR), lacY1, proC14, tsx-67, Δ(ompT-fepC)266, entA403, glnX44(AS), λ⁻, trpE38, rfbC1, rpsL109(strR), xylA5, mtl-1, thiE1) was used for the experiments. The host strain was transformed by the plasmid pSK004_SNAPtag_Arabinose (see SI part B for the plasmid map). The cells were typically grown in LB containing 50 μg/mL of carbenicillin at 37 °C and 200 rpm. Cultures were inoculated with 1:1000 (by volume) of an overnight pre-culture, and grown until OD_{600 nm} reached 0.35 at 37°C and 200 rpm. Half of the culture was induced with arabinose at a final concentration of 0.2 % for SNAP-tag expression. The cells were incubated for another hour

and then 1 mL of induced-culture ($OD_{600\text{ nm}}$ closed to 0.5) and the corresponding amount of non-induced cells (initial $OD_{600\text{ nm}}$ closed to 1.5, that is ca 1/3 mL collected) were washed twice in PBS (2x 300 μL).

Labeling of cells with fluorescent oligonucleotides

The cells (induced and non-induced) were resuspended in 50 μL PBS supplemented with 5 μM of fluorescent BG-modified oligonucleotide (BG-DNA₁-FAM or BG-DNA_{1c}-TAMRA). After 2 hours of incubation at 37°C in the dark, cells were washed thrice with PBS (3x 150 μL) by up-and-down pipetting, resuspended in 50 μL PBS and kept at 4°C overnight. Cells were then spotted (10 μL) on slides for microscopy analysis to verify the labelling efficiency. Images were firstly taken with a Zeiss Axioplan II epifluorescence microscope, using an QICAM Fast 1394 Digital Camera from QImaging and a 10x/0.30 Plan-Neofluar objective together with filters for DAPI, FITC (FAM) and rhodamine. Images were captured with Image Pro Express 6.0 and analyzed with FIJI softwares. Later in the project images were collected with a Zeiss Axio Observer 2.1 microscope with an ApoTome.2 imaging system using the Plan-Apochromat 20x/0,8 Ph2 M27 objective, an Hamamatsu Camera and different Zeiss filter sets (EGFP and DsRed). Three different slides were prepared for each condition and five micrographs were taken from each slide.

Cell viability

The cells (induced and non-induced) were resuspended in 50 μL PBS and incubated at 37°C for 2 hours. Cells were washed thrice with PBS by up-and-down pipetting, resuspended in 50 μL PBS and kept at 4°C overnight. Prior to propidium iodide (PI) staining, the volume of cells was adjusted to 1.5 mL with PBS and PI solution was then added to a final concentration of 1 μM . After 5 minutes of incubation, the samples were centrifuged 2 min at 4000 g, the supernatants were discarded and the pellets were resuspended in 50 μL PBS. Then 0.5 μL of 4,6-diamidino-2-phenylindole (DAPI) was added to a final concentration of 10 $\mu\text{g}/\text{mL}$. Cells were mounted on microscopic slides (10 μL) and observed after 5 min of incubation. Images were taken with a Zeiss Axioplan II epifluorescence microscope, using an QICAM Fast 1394 Digital Camera from QImaging and a 10x/0.30 Plan-Neofluar objective together with filters for DAPI and rhodamine. Images were captured with Image Pro Express 6.0. Three different slides were prepared for each condition and three micrographs were taken from each slide in fluorescence and brightfield. The data correspond to the means of three independent experiments. The total fluorescence was determined with FIJI software⁴⁶ and calculated as follow: corrected total cell fluorescence (CTCF) = Integrated Density – (Area of Selected picture x Mean Fluorescence of 3 Background readings). Then the fluorescence obtained with PI staining was divided by the total fluorescence obtained with DAPI staining to determine the percentage of dead cells.

Hybridization of oligonucleotides at the cell surface

The induced cells were resuspended in 50 μL PBS supplemented or not with 5 μM of non-fluorescent BG-modified oligonucleotide (BG-DNA_{1c} or BG-DNA₁). After an incubation at 37°C for 2 hours, cells were washed thrice with PBS by up-and-down pipetting, resuspended in 50 μL PBS and incubated with 50 μL of fluorescent oligonucleotides at 5 μM (respectively DNA₁-FAM or DNA_{1c}-TAMRA) for 5 min at 37°C. The cells were then washed once with

PBS (150 μL) by up-and-down pipetting, resuspended in 50 μL PBS and kept at 4°C overnight in the dark. Cells were mounted on microscopic slides (10 μL). Images were taken with a Zeiss Axioplan II epifluorescence microscope, using an QICAM Fast 1394 Digital Camera from QImaging and a 10x/0.30 Plan-Neofluar objective together with filters for DAPI, FITC (FAM) and rhodamine. Images were captured with Image Pro Express 6.0 and analyzed with FIJI softwares. At least five independent pictures were taken for each condition. The determination of total fluorescence area over total cells area in % using FIJI was performed by subtracting the light background (rolling ball radius 20 pixels) and setting the default auto thresholding for the phase contrast pictures and setting the default auto thresholding for DNA₁-FAM labelling and the auto thresholding using the Triangle algorithm for DNA_{1c}-TAMRA labelling in order to minimize the background fluorescence.

Enhancement of cell-cell tethering through modified oligonucleotides

Induced cells were resuspended in 50 μL PBS supplemented with 5 μM of BG-modified oligonucleotides (fluorescent oligonucleotides BG-DNA₁-FAM or BG-DNA_{1c}-TAMRA and non-fluorescent HNA oligonucleotides BG-HNA₁ or BG-HNA_{1c}). After an incubation at 37°C for 2 hours in the dark, cells were washed 4 times with PBS (4x 150 μL) by up-and-down pipetting, resuspended in 50 μL PBS and the two *E. coli* populations labeled with complementary oligonucleotides were mixed and incubated for an additional hour. Cells were then washed once with PBS (150 μL), resuspended in 100 μL PBS and kept at 4°C till overnight in the dark. Cells were spotted (10 μL) on slides for microscopy analysis and images were collected with a Zeiss Axio Observer 2.1 microscope with an ApoTome.2 imaging system using the Plan-Apochromat 20x/0,8 Ph2 M27 objective, an Hamamatsu Camera and different Zeiss filter sets (Phase, EGFP and DsRed). Three different slides were prepared for each condition and each slide was manually and visually completely scanned. When an aggregate was detected, then a picture was taken (11 pictures in mean per slide for DNA and 12 pictures in mean for HNA per slide). We used for comparison the single *E. coli* populations expressing one oligonucleotide at the surface (BG-DNA₁-FAM or BG-DNA_{1c}-TAMRA for DNA condition and non-fluorescent HNA oligonucleotides BG-HNA₁ or BG-HNA_{1c} for HNA condition). In these later conditions, 5 pictures were taken, mainly randomly. Aggregate areas were measured using the machine learning plug-in Trainable Weka Segmentation in FIJI. After training a classifier for aggregates, cells and background, input phase contrast pictures were segmented. The threshold was properly set for each probability maps obtained and particles areas above the size of 200 μm^2 were analyzed.

RESULTS

Design and synthesis of modified oligonucleotides

We deemed that the combination of SNAP-tag immobilization and the use of XNAs would i) improve the formation of cellular aggregates due to the formation of more stable HNA duplexes compared to dsDNA (ΔT_m of +1.3°C per base pair), ii) impart biostability due to the altered sugar chemistry which is of high relevance for *in vivo* applications, and iii) avoid unspecific anchoring of oligonucleotides into non-targeted cells which is the case for instance with lipid- or cholesterol-labelled sequences.⁴⁷

Protected *O*⁶-Benzylguanine phosphoramidite derivative was first synthesized (see Material and Methods for details) and used as precursor for the synthesis of modified oligonucleotides

(see Table 1). The oligonucleotides used in this study were 20-mer heterosequences designed to be long enough to avoid accessibility issues but also with a high GC-content (80%) to allow stable interactions with complementary counterparts (DNA_c or HNA_c) at 37°C. Two *O*⁶-benzylguanine containing DNA oligonucleotides were labeled with the fluorescent dyes 6-carboxyfluorescein (6-FAM) or carboxytetramethylrhodamine (TAMRA) at the 3' position to monitor correct binding to the SNAP-tag containing protein at the cell surface by fluorescence microscopy. The free energy of the DNA₁ and DNA_{1c} strands were calculated with nupack.org⁴⁸ using input parameters of 37°C with 140 mM NaCl. Despite the predominance of a high probable secondary structure ($\Delta G = -2.80$ kcal/mol and -2.21 kcal/mol respectively), UV-melting experiments confirmed the thermodynamic stability and prevalence of duplex formation over that of any type of potential secondary structure on each DNA single strand thus confirming the design of the sequences for mediating cell-cell aggregations (see SI part C).

<i>Designation</i>	<i>Sequences and modifications</i>
<i>BG-DNA₁-FAM</i>	5' <i>O</i> ⁶ -Benzylguanine-(PEG) ₄ -GCGCGAATTCCCCGGGCGCG-(6FAM)-3'
<i>BG-DNA_{1c}-TAMRA</i>	5' <i>O</i> ⁶ -Benzylguanine-(PEG) ₄ -CGCGCCCGGGGAATTTCGCGC-(TAMRA)-3'
<i>BG-DNA₁</i>	5' <i>O</i> ⁶ -Benzylguanine-(PEG) ₄ -GCGCGAATTCCCCGGGCGCG-3'
<i>BG-DNA_{1c}</i>	5' <i>O</i> ⁶ -Benzylguanine-(PEG) ₄ -CGCGCCCGGGGAATTTCGCGC-3'
<i>DNA₁-FAM*</i>	5'(FAM)-GCGCGAATTCCCCGGGCGCG-3'
<i>DNA_{1c}-TAMRA*</i>	5'(TAMRA)-CGCGCCCGGGGAATTTCGCGC-3'
<i>BG-HNA₁</i>	5' <i>O</i> ⁶ -Benzylguanine-(PEG) ₄ - GCGCGAATTCCCCGGGCGCG -3'
<i>BG-HNA_{1c}</i>	5' <i>O</i> ⁶ -Benzylguanine-(PEG) ₄ - CGCGCCCGGGGAATTTCGCGC -3'

* obtained from a commercial supplier

Table 1. Sequences of all synthesized DNA and HNA oligonucleotides used in this study

Labeling of cells with fluorescent oligonucleotides and cell viability

In order to ensure surface expression of sufficient amounts of the SNAP protein on *E. coli*, we employed the Maximized AutoTransporter Expression (MATE)-plasmid⁴⁹⁻⁵¹ pSK004_SNAPtag_Arabinose which encodes for fusion proteins consisting of the *N*-terminal CtxB signal peptide (SP) from *Vibrio cholerae*, followed by gene SNAP26b which is a mutant form of the human gene for *O*⁶-alkylguanine-DNA-alkyltransferase (hAGT) and the translocator domain of the EhaA autotransporter from *E. coli* under the control of an Arabinose-inducible promoter. (Figure 2a)

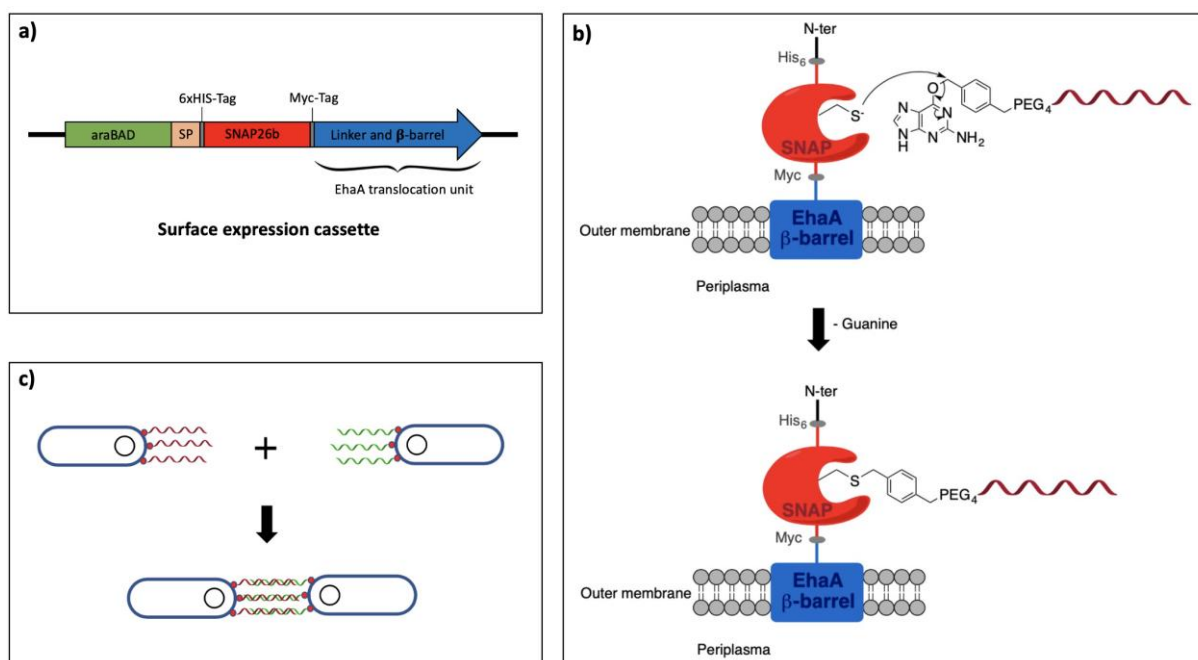


Figure 2. pSK004_SNAPtag_Arabinose, the corresponding fusion protein expressed on the bacterial surface and expected interactions at the cell level. a) Schematic representation of the surface expression vector pSK004_SNAPtag_Arabinose based on the EhaA autotransporter adapted from Schulte *et al.*⁴⁹. Expression is under the control of the araBAD promoter, followed by a signal peptide SP and two detection tags (His6 and Myc) flanking the passenger protein, i.e. the SNAP26 protein. b) Scheme highlighting the matured fusion protein at the cell surface from vector pSK004_SNAPtag_Arabinose and labelling mechanism of SNAP- tag. c) Representation of cellular aggregation mediated by hybridization of complementary single stranded oligonucleotides. This schematic representation does not reflect the real SNAP partitioning on the cell surface.

We deemed this design to be adequate for triggering XNA-mediated cellular aggregation since it has been shown that the autotransporter EhaA which contributes to adhesion, colonization and biofilm formation by enterohemorrhagic *E. coli* O157:H7⁵² was suitable for surface display not only in *E. coli*,⁵³ but also in other bacteria.⁵⁴ In addition, the SNAP- tag engineered by Johnsson and colleagues can specifically and covalently bind *O*⁶-benzylguanine (BG) derivatives thus enabling covalent attachment of oligonucleotides on cell surfaces.⁵⁵ Next, the OmpT-negative host strain *E. coli* UT5600 (DE3) was transformed with this MATE-plasmid (pSK004_SNAPtag_Arabinose) to express the SNAP proteins at the surface after arabinose induction. Induction of the SNAP proteins expression at the cell surface was controlled by microscopy analysis after incubation of the induced cells with the commercially available SNAP-Surface Alexa Fluor dye 488 for 30 min (data not shown). In order to evaluate whether oligonucleotides could be immobilized by the SNAP tags on the surface of cells (Figure 2b), we incubated cells with the fluorescent BG-oligonucleotides BG-DNA₁-FAM or BG-DNA_{1c}-TAMRA (Table 1) to covalently fix them to SNAP proteins by application of an adapted protocol by Merlo *et al.*⁵⁶ After incubation with the fluorescently-labelled oligonucleotides, the cells were subjected to fluorescence microscopy. This analysis revealed that the incubation time needed to be adjusted to the presence of the TAMRA fluorophore since a 30 min incubation time was not sufficient to produce any fluorescent labelling of cells. When the incubation time was increased to 2h,⁵⁷ the expected fluorescence staining with TAMRA-containing oligonucleotides was obtained (Figure 3). On

the other hand, FAM-labeled DNA showed detectable but greatly reduced fluorescence intensity compared to TAMRA staining probably due to fluorescence quenching by the proximal guanine base at the 3'-position (Figure 3).⁵⁸ Overall, this fluorescence microscopy analysis revealed that only modified cells became fluorescent after induction, and as expected no fluorescence was detected on non-induced cells.

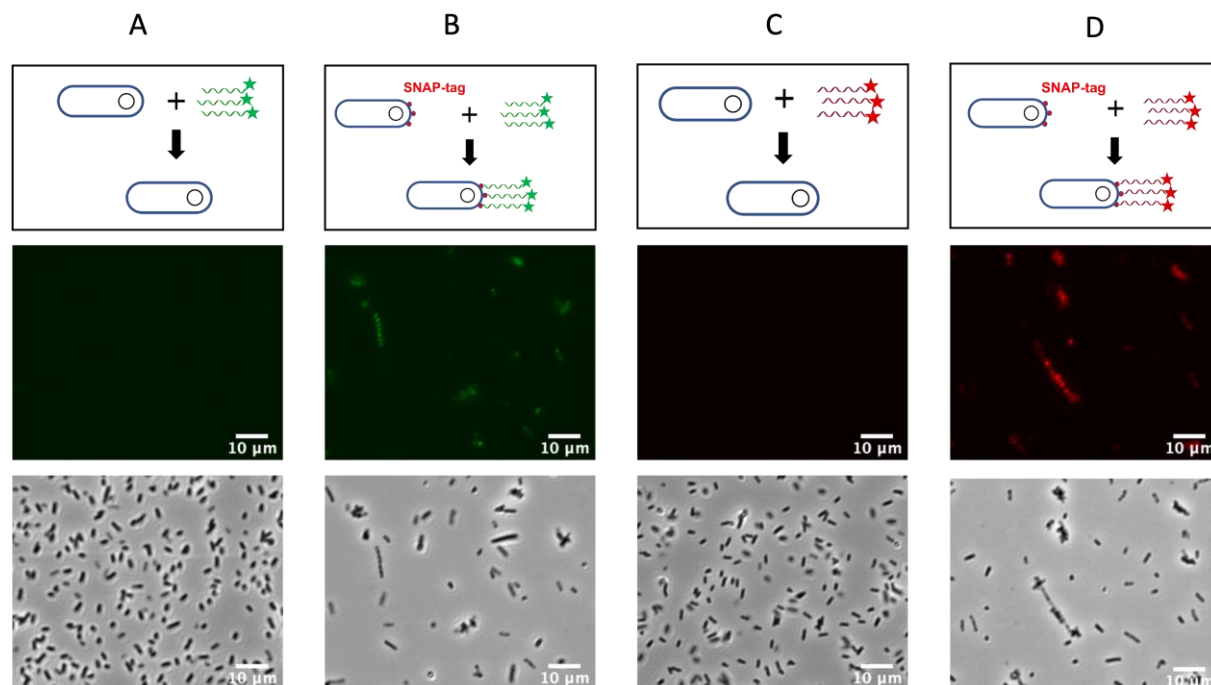


Figure 3. Fluorescence microscopy analysis of *E. coli* cells labeled with BG-DNA₁-FAM (B) and BG-DNA_{1c}-TAMRA (D). The corresponding staining was applied on SNAP-expressing cells (B and D) and SNAP-non expressing cells as negative controls (A and C). Each fluorescence picture is appended with its corresponding brightfield below. The fluorescence micrographs were colored using the FIJI LUT tool and no background correction was applied. All micrographs were automatically adjusted for brightness and contrast using FIJI.

We also examined the viability of the cells after overexpression of this SNAP cell surface system. The cells were treated in the same conditions as for the experiments except that no fluorescent oligonucleotides were added. After treatment of the samples with 4,6-diamidino-2-phenylindole (DAPI) to identify live and dead cells and propidium iodide (PI) at 1 µM to identify dead cells, the fluorescence of randomly selected micrographs was quantified (Figure 4). We did not increase the final concentration of the PI working solution above 1 µM as we noticed a toxic effect at higher concentrations.⁶¹ We observed a two times higher ratio of PI-stained cells compared to DAPI-stained cells after arabinose induction, namely 8.3% dead cells when the SNAP system was over expressed versus 3.6% dead cells without overexpression. Thus, the SNAP system expressed at the surface of *E. coli* does not induce substantial cytotoxic effect in those conditions.

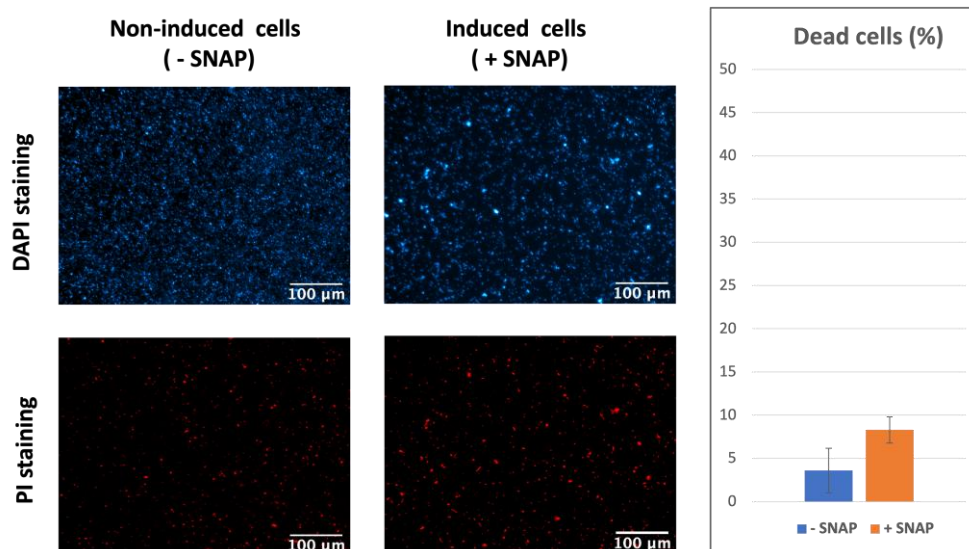


Figure 4. Viability of *E. coli* after SNAP-tag induction at the cell surface. *E. coli* cells induced or not with arabinose were treated under the same experimental conditions and co-stained with DAPI and PI. Fluorescence micrographs were colored post-acquisition, and the brightness and contrast were adjusted in FIJI for illustration. Relative fluorescence was quantified, and data are presented as mean values \pm SD of 9 pictures of three independent experiments (see Materials and Methods for details).

Hybridization of oligonucleotides at the cell surface

We next sought to demonstrate the possibility of binding cells through DNA by simple hybridization events of complementary oligonucleotides located on the cell surface. To do so, we attached the non-fluorescent oligonucleotides BG-DNA₁ or BG-DNA_{1c} on to cells by a similar protocol as described previously and after washing, we co-incubated these cells with complementary, fluorescently labelled oligonucleotides (i.e. DNA_{1c}-TAMRA and DNA₁-FAM, respectively). Expectedly, no staining was observed with cells that did not display BG-DNA_{1c} on the cell surface but that were incubated with DNA₁-FAM thus clearly indicating the necessity and the specificity of the hybridization step (Figure 5A & 5B). Intriguingly, when the SNAP-induced cells were not incubated with BG-DNA₁, the fluorescence emission of the DNA_{1c}-TAMRA oligonucleotide was equivalent to that of cells expressing BG-DNA₁ at their surface (*vide infra*). Surprisingly, the reduction of the time of incubation from one hour to five minutes and the number of washes after hybridization (from three to one), allowed to restore the expected difference of TAMRA fluorescence emission between the negative control and samples obtained under hybridization conditions (Figure 5C&5D and E right bars). For quantification of cell aggregates, we opted to express fluorescence area relative to cells area for a given micrograph to quantify the level of labelling and thus cell areas capable of hybridizing with other cells. Indeed, working with motile non-immobilized live cells can lead to the observation of cells that do not belong to the same focal plane and that can overlap or adopt different 3D-orientations. At low magnification, it is particularly difficult to set the outlines of the cells as well as the non-homogenous staining of a single cell and the filamentous phenotype displayed by some cells did not allow the determination of a precise ratio of fluorescent cells relative to the total number of cells.

After induction of the SNAP-tag, around 51% of all cell surfaces conjugated to BG-DNA_{1c} were fluorescent after incubation with DNA₁-FAM compared to only ca 3% of all cell surfaces lacking BG-DNA_{1c} (Figure 5E left bars). As mentioned before, we observed a high unspecific signal with the TAMRA-labelled oligonucleotide since we observed a ca 38% of fluorescence area relative to cells area after incubation of cells with BG-DNA₁ with the

complementary fluorescent DNA_{1c}-TAMRA but also ca 27% of fluorescence area for cells that did not exhibit any oligonucleotide covalently linked to the SNAP-tag (Figure 5E right bars). This rather high background fluorescence may be ascribed to the fact that the TAMRA fluorophore consists of two regioisomers (see SI part D), and only the 5-positional regioisomer displays a significantly higher background fluorescence than the corresponding 6-carboxyrhodamines when used as SNAP-tag substrates for fluorescence labelling in live cells.⁶² The DNA_{1c}-TAMRA oligonucleotide obtained from a commercial supplier contained predominantly the 5-regioisomer of the dye because the 5-regioisomers often display higher quantum yields than 6-regioisomers when conjugated⁶³ but this also explains the high background observed for the negative control with the TAMRA-labelled oligonucleotide. Based on these observations, we thus synthesized the modified BG-DNA_{1c}-TAMRA oligonucleotide with the 6-regioisomer of the TAMRA fluorophore.

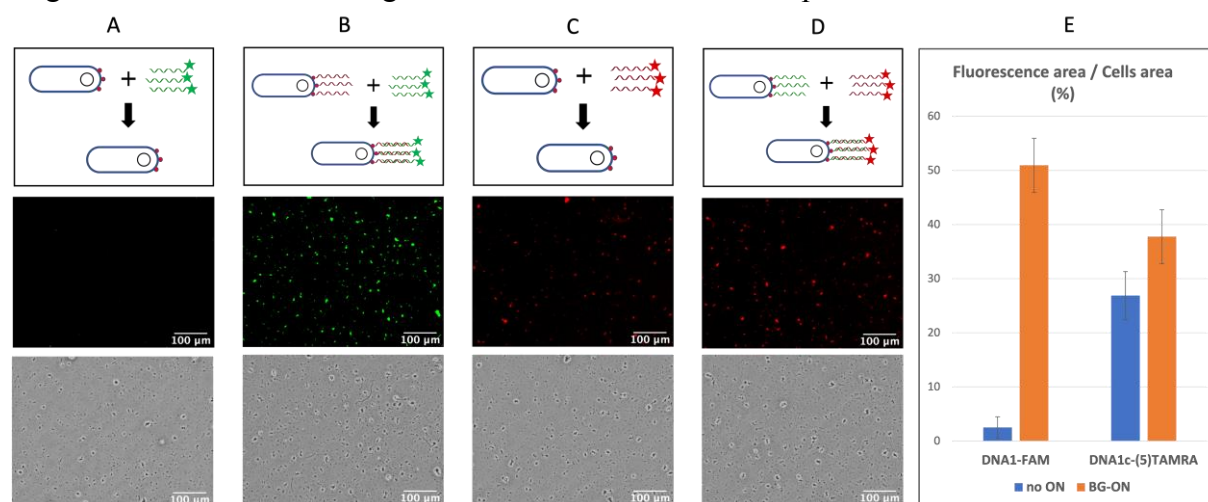


Figure 5. Hybridization of fluorescent oligonucleotides (ON) with complementary counterpart exposed at the cell surface of *E. coli*. Experimental scheme, fluorescence and bright field micrographs of DNA₁-FAM (green) at 5 μ M incubated with *E. coli* cells exposing solely the SNAP-tag ('no ON' condition for no complementary oligonucleotide immobilized at the cell surface) or pretreated with 5 μ M BG-DNA_{1c} (red) linked to the SNAP-tag (columns A and B). DNA_{1c}-TAMRA (red) at 5 μ M was also incubated with *E. coli* cells exposing solely the SNAP-tag ('no ON' condition for no complementary oligonucleotide immobilized at the cell surface) or pretreated with 5 μ M BG-DNA₁ (green) linked to the SNAP-tag (columns C and D). Fluorescence micrographs were colored post-acquisition, phase contrast pictures smoothed using FFT bandpass filter in FIJI and the brightness and contrast were adjusted for illustration as well. Relative fluorescence was quantified using FIJI software. Data are presented as mean values \pm SD of at least 5 pictures (histogram E).

Enhancement of cell-cell tethering with DNA and XNA oligonucleotides

With the SNAP-tag installed as a cell surface decorating system, we explored the possibility of self-assembly of multicellular aggregates through complementary DNA hybridization (Figure 2c). We mixed two populations of *E. coli*, each of them displaying at the cell surface oligonucleotide BG-DNA₁-FAM or BG-DNA_{1c}-TAMRA. The analyses were achieved at the microscopic scale on non-immobilized cells at the lowest possible magnification of the microscope to increase the probability of visualizing rare objects. As expected, we observed the formation of aggregates made of cells with DNA₁-FAM and DNA_{1c}-TAMRA at the surface with different morphologies and different sizes (Figure 6).

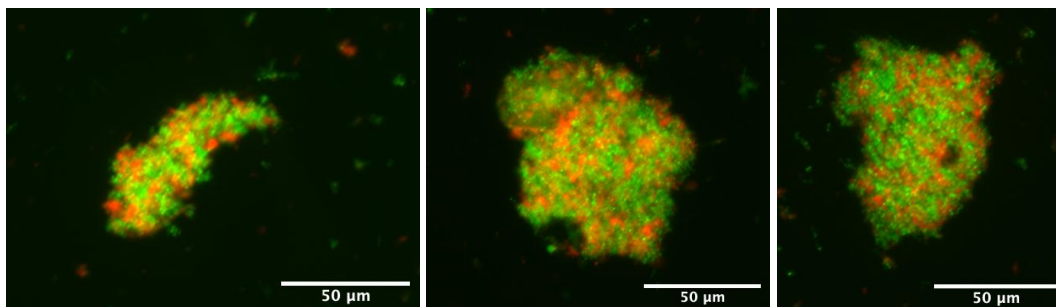


Figure 6. Illustrative *E. coli* aggregates via Watson-Crick base pairing. 1:1 mixture of two *E. coli* populations each of them labeled with a fluorescent and complementary sequence at their surface BG-DNA₁-FAM in green and BG-DNA_{1c}-TAMRA in red. They illustrate the quantification results from Figure 7 where two cell populations with complementary DNA oligonucleotides were mixed together (left panel, blue columns). Fluorescence micrographs were colored post-acquisition and presented as composite images using FIJI.

The aggregates were resistant to breakage through multiple physical pipetting during sample preparation and were observed to be essentially static structures over the timescale of microscopy acquisition which allowed straightforward quantification. Surprisingly, we could also observe very small aggregates in the control conditions that are, induced cells without any oligonucleotides at the surface (data not shown) and induced cells with only one oligonucleotide displayed at the surface. The aggregates were counted, and their area determined using the machine learning plug-in Trainable Weka Segmentation in FIJI. After exclusion of aggregates that were not totally composed of cells or that did not belong to the focal plane (see in SI part E), we ranked them according to their apparent area expressed in μm^2 (Figure 7a). When separate cell populations decorated with complementary oligonucleotides BG-DNA₁-FAM or BG-DNA_{1c}-TAMRA were mixed together, we observed a marked enhancement of cell-cell tethering reflected by the number of aggregates (blue column) compared to the control conditions (orange and grey columns respectively for BG-DNA₁-FAM and BG-DNA_{1c}-TAMRA expressing cells) especially for the smaller aggregates (size between 200 and 700 μm^2 , ca 4 and 8 times more) and the larger ones ($> 2700 \mu\text{m}^2$, ca 8 times more and 11 aggregates versus zero for population with only BG-DNA_{1c}-TAMRA at the surface). We performed the same experiment but with unnatural HNA oligonucleotides (Figure 7b). In this case, we also could observe a marked increase in the number of aggregates when the two different *E. coli* populations were incubated together, especially for the smaller and larger aggregates. We observed the formation of ca 23 time more aggregates with a size between 200 and 700 μm^2 when the cells interacted via two complementary HNA oligonucleotides (blue column) compared to the cells with only the BG-HNA_{1c} at the surface and ca 8 times more aggregates compared to the cells with only the BG-HNA₁. For the larger aggregates ($> 2700 \mu\text{m}^2$), there were ca 19 and 6 times more aggregates compared to cells with solely BG-HNA_{1c} and BG-HNA₁ (grey and orange columns, respectively). Moreover, comparing the results obtained with DNA and HNA oligonucleotides, we observed overall more aggregates with the HNAs, in particular for the small aggregates (200-700 μm^2 , approximately twice as much with the HNAs). This can be explained by the higher stability of the HNA duplexes compared to natural dsDNA that makes the aggregates more difficult to dissociate.⁶⁴ Regardless whether DNA or HNA oligonucleotides were used, the size and the shape of the aggregates varied strongly.

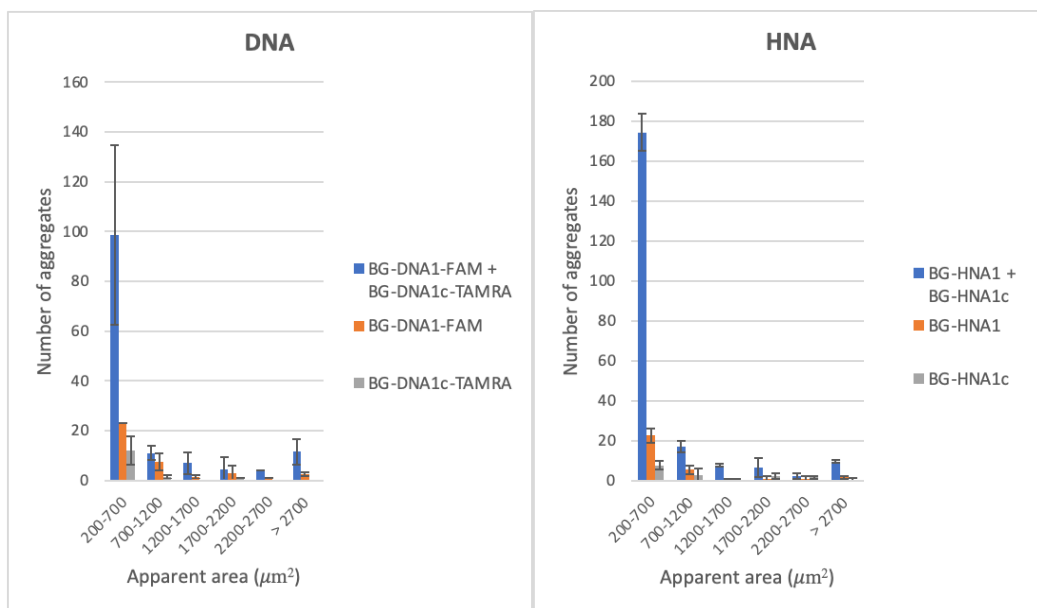


Figure 7. Quantification of the aggregates obtained after base pairing of natural and non-natural oligonucleotides. Brightfield micrographs of cell aggregates obtained after hybridization of DNA or HNA complementary oligonucleotides exposed at the cell surface of two different cell populations were analyzed. The plugin Trainable Weka Segmentation in FIJI software allowed us to create binary pictures of which particles surfaces were measured and ranked into size ranges. Data are shown as mean \pm SD of two independent biological experiments.

Lastly, we observed that the green fluorescence (FAM) or red fluorescence (TAMRA) of complementary BG-DNA sequences, was not equally distributed on the entire surface of the aggregates. After mixing the two cell populations for attachment, yellow fluorescence was observed locally, while green and red fluorescence were still observed on the cell surfaces probably due to the preorganization of the aggregates in smaller structures as observed for cells equipped with a single fluorescent oligonucleotide at the surface. Moreover, FAM and TAMRA dyes are frequently used in tandem as the FAM fluorescence may be quenched by TAMRA when located in close proximity through Förster resonance energy transfer (FRET). The degree of the FRET effect was quantified through micrographs analysis (see SI part F) and an average of 46% FAM fluorescence decrease was determined in presence of TAMRA exposing cells. This partial FRET effect may be due to preorganization of the cells in smaller aggregates as in cells with only one fluorescent oligonucleotide at the surface.

DISCUSSION

SNAP-tag to mediate covalent binding of oligonucleotides on cell surfaces

The heterogeneity of biological membranes as well as the range of applications justify the continuous development of conjugation methods for the integration of various biomaterials at the cell surface. In this work, we reengineered *E. coli* to covalently bind DNA and HNA oligonucleotides at the cell surface through the SNAP-tag protein. We first validated the accessibility of the extracellular SNAP protein by covalently linking the commercially available SNAP-Surface Alexa Fluor dye 488 and BG-modified oligonucleotides labelled with two fluorophores (FAM and TAMRA) at the 3' termini. This system led to a robust, fluorescent staining as all the microscopy experiments were carried out one day after the

labelling. In addition, no internalization of the modified oligonucleotides was observed as hybridization with complementary fluorescent oligonucleotides revealed the persistence of the BG-modified oligonucleotides at the cell surface. When this robust surface modification method was applied to two distinct cell populations, numerous and large aggregates were formed after SNAP expression induction. Importantly, HNA displayed a higher capacity at mediating cellular aggregation than canonical DNA.

On a practical point of view, microscopy observations were done on non-fixed live cells which made the analysis easier and faster. We measured the mean fluorescence intensity from a large population of cells (in the 10^8 range) by analyzing micrographs taken with a low magnification objective to minimize the variation in fluorescence at the individual cell level. We were then able to quantify cell surface staining and characterize aggregation (number and size of aggregates) while being able to have a close look on the phenotype of the cells at the same time. It is obvious that this type of analysis allows a non-exhaustive but rapid evaluation of a mode of conjugation of biomolecules on the surface of cells since observations are made in two rather than in three dimensions.

The system we used to decorate cells relies on a genetic approach. The expression at the cell surface of the SNAP-tag protein allows a highly specific conjugation with BG-containing nucleic acid molecules. It is stable in physiological conditions, and easy to use once the cells have been engineered with the proper plasmid. In addition, we described for the first time the effect of SNAP-tag expression at the cell surface of *E. coli* in terms of cell viability. We did not observe any significant toxicity under our experimental conditions. Nonetheless, it is worth mentioning that we observed the formation of a filamentous phenotype which occurs by the elongation of the cells with more than one septum due to incomplete cell division. We could also observe that the staining was not homogeneously distributed at the surface of the cells. While similar morphological difference have been reported for other receptor systems,⁵⁹ additional experiments such as DNA-PAINT or super-resolution confocal microscopy will be required to identify the origin of this non-homogenous protein expression.

The role of XNAs in cellular aggregation

We combined the exposure of the SNAP protein at *E. coli* cell surface with the conjugation of oligonucleotides. The advantages of using modified oligonucleotides as SNAP binders include the ability to precisely control the orientation, distances, and valency of these binders.⁶⁵⁻⁶⁷ Moreover these biomaterials could allow to fine-tune cell-cell distance as their length is highly adaptable. We showed in this work that even short heterosequences (20-mer) led to stable aggregates. Besides, oligonucleotides tethering can be easily abolished by enzymatic treatment or strand displacement even in complex assembled structures or modulated to increase the stability of the duplexes.^{3, 37,41,68} Thus, the association of the SNAP protein and modified oligonucleotides at *E. coli* surface is able to provide a highly specific system with a dynamic control of interactions and unlimited combinations of interactions through complementary oligonucleotides. Beyond the added value of mediating cellular interactions with oligonucleotides equipped with BG moieties, we have included a second layer of chemical modifications by altering the sugar chemistry of oligonucleotides. Indeed, the appendage of fully modified HNA sequences on cell surfaces could protect oligonucleotides against nuclease degradation⁶⁹ and also ensures orthogonality with natural DNA and RNA; feats that are difficult to achieve with canonical systems or other, more simple sugar modifications. Such an approach can be expanded to yet more orthogonal XNA systems such as homo-DNA ((4' to 6')-linked oligo-2',3'-dideoxy-beta-D-glucopyranose nucleic acid) or 3'-2' phosphonomethyl-threosyl nucleic acid (tPhoNA).^{70,71}

On a technical point of view, the grafting of nucleic acids at the cell surface can significantly improve the intensity of the cells staining with intercalating dyes as observed in our study with DAPI (data not shown) and more broadly can provide tools to increase brightness in fluorescence microscopy in a controlled manner.³⁹ Artificial bacterial aggregation through nucleic acids has a broad range of applications. It could allow the study of biofilm formation and the advantages that this spatial organization confers to bacteria, such as protection against antibiotics for example or to help unravelling the mechanisms of formation of biofilms.⁷² Other potential, direct applications include the investigation of molecular signals involved in a quorum sensing processes upon reaching a certain threshold population density and the analysis of the symbiotic relationship in gut microbiota. Finally, it could contribute to the creation of artificial bacterial communities and/or engineer synergistic multicellular metabolic pathways to improve the biosynthesis efficiency of a desired product.⁷³

CONCLUSIONS

The methods developed in this work to expose synthetic genetic materials especially HNA at the cell surface are leading to bio-orthogonal bacteria–bacteria interactions. In this context, surface molecules must be provided exogenously and continuously to avoid dilution during bacterial division which is an asset for safety concerns. In this work, aggregation was observed starting from homotypic cells but this system may be easily generalize to heterotypic cells.

ACKNOWLEDGEMENTS

We would like to thank Dr. Jacob Seeler and Pr. Anne Dejean (Pasteur Institute, Paris) for giving us the opportunity to have access to the Apotome Zeiss microscope. We would also like to thank Dr. Valérie Pezo for making the facilities available to carry out the work.

FUNDING : University of Evry-Val-d’Essonne and ERC-AG (FP7-320683).

- (1) Rogozhnikov, D.; O'Brien, P. J.; Elahipanah, S.; Yousaf, M. N. Scaffold Free Bio-Orthogonal Assembly of 3-Dimensional Cardiac Tissue via Cell Surface Engineering. *Scientific Reports* **2016**, *6*. <https://doi.org/10.1038/srep39806>.
- (2) Gartner, Z. J.; Bertozzi, C. R. Programmed Assembly of 3-Dimensional Microtissues with Defined Cellular Connectivity. *Proceedings of the National Academy of Sciences of the United States of America* **2009**, *106* (12), 4606–4610. <https://doi.org/10.1073/pnas.0900717106>.
- (3) Todhunter, M. E.; Jee, N. Y.; Hughes, A. J.; Coyle, M. C.; Cerchiari, A.; Farlow, J.; Garbe, J. C.; LaBarge, M. A.; Desai, T. A.; Gartner, Z. J. Programmed Synthesis of Three-Dimensional Tissues. *Nature Methods* **2015**, *12* (10), 975–981. <https://doi.org/10.1038/nmeth.3553>.
- (4) Gong, P.; Zheng, W.; Huang, Z.; Zhang, W.; Xiao, D.; Jiang, X. A Strategy for the Construction of Controlled, Three-Dimensional, Multilayered, Tissue-like Structures. *Advanced Functional Materials* **2013**, *23* (1), 42–46. <https://doi.org/10.1002/adfm.201201275>.
- (5) Pulsipher, A.; Griffin, M. E.; Stone, S. E.; Hsieh-Wilson, L. C. Long-Lived Engineering of Glycans to Direct Stem Cell Fate. *Angewandte Chemie - International Edition* **2015**, *54* (5), 1466–1470. <https://doi.org/10.1002/anie.201409258>.
- (6) Zhao, W.; Loh, W.; Droujinine, I. A.; Teo, W.; Kumar, N.; Schafer, S.; Cui, C. H.; Zhang, L.; Sarkar, D.; Karnik, R.; Karp, J. M. Mimicking the Inflammatory Cell Adhesion Cascade by Nucleic Acid Aptamer Programmed Cell- cell Interactions. *The FASEB Journal* **2011**, *25* (9), 3045–3056. <https://doi.org/10.1096/fj.10-178384>.
- (7) Morsut, L.; Roybal, K. T.; Xiong, X.; Gordley, R. M.; Coyle, S. M.; Thomson, M.; Lim, W. A. Engineering Customized Cell Sensing and Response Behaviors Using Synthetic Notch Receptors. *Cell* **2016**, *164* (4). <https://doi.org/10.1016/j.cell.2016.01.012>.
- (8) Shi, P.; Ju, E.; Yan, Z.; Gao, N.; Wang, J.; Hou, J.; Zhang, Y.; Ren, J.; Qu, X. Spatiotemporal Control of Cell-Cell Reversible Interactions Using Molecular Engineering. *Nature Communications* **2016**, *7*. <https://doi.org/10.1038/ncomms13088>.
- (9) Ko, I. K.; Kean, T. J.; Dennis, J. E. Targeting Mesenchymal Stem Cells to Activated Endothelial Cells. *Biomaterials* **2009**, *30* (22), 3702–3710. <https://doi.org/10.1016/j.biomaterials.2009.03.038>.
- (10) Sugimoto, S.; Moriyama, R.; Mori, T.; Iwasaki, Y. Surface Engineering of Macrophages with Nucleic Acid Aptamers for the Capture of Circulating Tumor Cells. *Chemical Communications* **2015**, *51* (98), 17428–17430. <https://doi.org/10.1039/c5cc06211j>.
- (11) Sun, L.; Shen, F.; Xu, J.; Han, X.; Fan, C.; Liu, Z. DNA- Edited Ligand Positioning on Red Blood Cells to Enable Optimized T Cell Activation for Adoptive Immunotherapy. *Angew. Chem. Int. Ed.* **2020**, *59* (35), 14842–14853. <https://doi.org/10.1002/anie.202003367>.
- (12) Shi, P.; Ju, E.; Wang, J.; Yan, Z.; Ren, J.; Qu, X. Host–Guest Recognition on Photo-Responsive Cell Surfaces Directs Cell–Cell Contacts. *Materials Today* **2017**, *20* (1), 16–21. <https://doi.org/10.1016/j.mattod.2016.12.006>.
- (13) Neu, B.; Meiselman, H. J. Depletion-Mediated Red Blood Cell Aggregation in Polymer Solutions. *Biophysical Journal* **2002**, *83* (5). [https://doi.org/10.1016/S0006-3495\(02\)75259-4](https://doi.org/10.1016/S0006-3495(02)75259-4).
- (14) Csizmar, C. M.; Petersburg, J. R.; Wagner, C. R. Programming Cell-Cell Interactions through Non-Genetic Membrane Engineering. *Cell Chemical Biology* **2018**, *25* (8), 931–940. <https://doi.org/10.1016/j.chembiol.2018.05.009>.
- (15) Kong, Y.; Du, Q.; Li, J.; Xing, H. Engineering Bacterial Surface Interactions Using DNA as a Programmable Material. *Chemical communications (Cambridge, England)* **2022**, *58* (19), 3086–3100. <https://doi.org/10.1039/d1cc06138k>.
- (16) Ma, J.; Wang, Y.; Huang, Y.; Zhang, Y.; Cui, Y.; Kong, D. Chemical–Biological

- Approaches for the Direct Regulation of Cell–Cell Aggregation. *Aggregate* **2022**, *3* (2). <https://doi.org/10.1002/agt2.166>.
- (17) Saxon, E.; Bertozzi, C. R. Cell Surface Engineering by a Modified Staudinger Reaction. *Science* **2000**, *287* (5460), 2007–2010. <https://doi.org/10.1126/science.287.5460.2007>.
- (18) Glass, D. S.; Riedel-Kruse, I. H. A Synthetic Bacterial Cell-Cell Adhesion Toolbox for Programming Multicellular Morphologies and Patterns. *Cell* **2018**, *174* (3), 649–658.e16. <https://doi.org/10.1016/j.cell.2018.06.041>.
- (19) Chen, B.; Kang, W.; Sun, J.; Zhu, R.; Yu, Y.; Xia, A.; Yu, M.; Wang, M.; Han, J.; Chen, Y.; Teng, L.; Tian, Q.; Yu, Y.; Li, G.; You, L.; Liu, Z.; Dai, Z. Programmable Living Assembly of Materials by Bacterial Adhesion. *Nature Chemical Biology* **2022**, *18* (3), 289–294. <https://doi.org/10.1038/s41589-021-00934-z>.
- (20) Veiga, E.; De Lorenzo, V.; Fernández, L. A. Autotransporters as Scaffolds for Novel Bacterial Adhesins: Surface Properties of Escherichia Coli Cells Displaying Jun/Fos Dimerization Domains. *Journal of Bacteriology* **2003**, *185* (18), 5585–5590. <https://doi.org/10.1128/JB.185.18.5585-5590.2003>.
- (21) Kozlowski, M. T.; Silverman, B. R.; Johnstone, C. P.; Tirrell, D. A. Genetically Programmable Microbial Assembly. *ACS Synthetic Biology* **2021**, *10* (6), 1351–1359. <https://doi.org/10.1021/acssynbio.0c00616>.
- (22) Chao, G.; Wannier, T. M.; Gutierrez, C.; Borders, N. C.; Appleton, E.; Chadha, A.; Lebar, T.; Church, G. M. HelixCAM: A Platform for Programmable Cellular Assembly in Bacteria and Human Cells. *Cell* **2022**, *185* (19), 3551–3567.e39. <https://doi.org/10.1016/j.cell.2022.08.012>.
- (23) Chen, F.; Warnock, R. L.; Van Der Meer, J. R.; Wegner, S. V. Bioluminescence-Triggered Photoswitchable Bacterial Adhesions Enable Higher Sensitivity and Dual-Readout Bacterial Biosensors for Mercury. *ACS Sensors* **2020**, *5* (7), 2205–2210. <https://doi.org/10.1021/acssensors.0c00855>.
- (24) Chen, F.; Wegner, S. V. Blue-Light-Switchable Bacterial Cell-Cell Adhesions Enable the Control of Multicellular Bacterial Communities. *ACS Synthetic Biology* **2020**, *9* (5), 1169–1180. <https://doi.org/10.1021/acssynbio.0c00054>.
- (25) Peschke, T.; Rabe, K. S.; Niemeyer, C. M. Orthogonal Surface Tags for Whole-Cell Biocatalysis. *Angewandte Chemie - International Edition* **2017**, *56* (8). <https://doi.org/10.1002/anie.201609590>.
- (26) Gallus, S.; Peschke, T.; Paulsen, M.; Burgahn, T.; Niemeyer, C. M.; Rabe, K. S. Surface Display of Complex Enzymes by in Situ SpyCatcher-SpyTag Interaction. *ChemBioChem* **2020**, *21* (15), 2126–2131. <https://doi.org/10.1002/cbic.202000102>.
- (27) Feng, L.; Gao, L.; Sauer, D. F.; Ji, Y.; Cui, H.; Schwaneberg, U. Fe(II)-Complex Mediated Bacterial Cell Surface Immobilization of EGFP and Enzymes. *Chemical Communications* **2021**, *57* (36), 4460–4463. <https://doi.org/10.1039/d1cc01575c>.
- (28) Shi, P.; Zhao, N.; Lai, J.; Coyne, J.; Gaddes, E. R.; Wang, Y. Polyvalent Display of Biomolecules on Live Cells. *Angew. Chem. Int. Ed.* **2018**, *57* (23), 6800–6804. <https://doi.org/10.1002/anie.201712596>.
- (29) Ge, Z.; Liu, J.; Guo, L.; Yao, G.; Li, Q.; Wang, L.; Li, J.; Fan, C. Programming Cell-Cell Communications with Engineered Cell Origami Clusters. *Journal of the American Chemical Society* **2020**, *142* (19), 8800–8808. <https://doi.org/10.1021/jacs.0c01580>.
- (30) Weber, R. J.; Liang, S. I.; Selden, N. S.; Desai, T. A.; Gartner, Z. J. Efficient Targeting of Fatty-Acid Modified Oligonucleotides to Live Cell Membranes through Stepwise Assembly. *Biomacromolecules* **2014**, *15* (12), 4621–4626. <https://doi.org/10.1021/bm501467h>.
- (31) Taylor, M. J.; Husain, K.; Gartner, Z. J.; Mayor, S.; Vale, R. D. A DNA-Based T Cell

- Receptor Reveals a Role for Receptor Clustering in Ligand Discrimination. *Cell* **2017**, *169* (1), 108-119.e20. <https://doi.org/10.1016/j.cell.2017.03.006>.
- (32) Nieves, D. J.; Hilzenrat, G.; Tran, J.; Yang, Z.; MacRae, H. H.; Baker, M. A. B.; Gooding, J. J.; Gaus, K. TagPAINT: Covalent Labelling of Genetically Encoded Protein Tags for DNA-PAINT Imaging. *Royal Society Open Science* **2019**, *6* (12), 191268. <https://doi.org/10.1098/rsos.191268>.
- (33) Yao, L.; Zhang, L.; Fei, Y.; Chen, L.; Mi, L.; Ma, J. Application of SNAP-Tag in Expansion Super-Resolution Microscopy Using DNA Oligostrands. *Front Chem* **2021**, *9*, 640519. <https://doi.org/10.3389/fchem.2021.640519>.
- (34) Tian, Q.; Bagheri, Y.; Keshri, P.; Wu, R.; Ren, K.; Yu, Q.; Zhao, B.; You, M. Efficient and Selective DNA Modification on Bacterial Membranes. *Chemical Science* **2021**, *12* (7), 2629–2634. <https://doi.org/10.1039/d0sc06630c>.
- (35) Twite, A. A.; Hsiao, S. C.; Onoe, H.; Mathies, R. A.; Francis, M. B. Direct Attachment of Microbial Organisms to Material Surfaces Through Sequence-Specific DNA Hybridization. *Adv. Mater.* **2012**, *24* (18), 2380–2385. <https://doi.org/10.1002/adma.201104336>.
- (36) Furst, A. L.; Smith, M. J.; Lee, M. C.; Francis, M. B. DNA Hybridization to Interface Current-Producing Cells with Electrode Surfaces. *ACS Central Science* **2018**, *4* (7), 880–884. <https://doi.org/10.1021/acscentsci.8b00255>.
- (37) Gao, T.; Chen, T.; Feng, C.; He, X.; Mu, C.; Anzai, J. ichi; Li, G. Design and Fabrication of Flexible DNA Polymer Cocoons to Encapsulate Live Cells. *Nature Communications* **2019**, *10* (1). <https://doi.org/10.1038/s41467-019-10845-2>.
- (38) Mela, I.; Vallejo-Ramirez, P. P.; Makarchuk, S.; Christie, G.; Bailey, D.; Henderson, R. M.; Sugiyama, H.; Endo, M.; Kaminski, C. F. DNA Nanostructures for Targeted Antimicrobial Delivery. *Angewandte Chemie - International Edition* **2020**, *59* (31), 12698–12702. <https://doi.org/10.1002/anie.202002740>.
- (39) Geng, Z.; Cao, Z.; Liu, R.; Liu, K.; Liu, J.; Tan, W. Aptamer-Assisted Tumor Localization of Bacteria for Enhanced Biotherapy. *Nature Communications* **2021**, *12* (1). <https://doi.org/10.1038/s41467-021-26956-8>.
- (40) Lahav-Mankovski, N.; Prasad, P. K.; Oppenheimer-Low, N.; Raviv, G.; Dadosh, T.; Unger, T.; Salame, T. M.; Motiei, L.; Margulies, D. Decorating Bacteria with Self-Assembled Synthetic Receptors. *Nature Communications* **2020**, *11* (1). <https://doi.org/10.1038/s41467-020-14336-7>.
- (41) Gavins, G. C.; Gröger, K.; Bartoschek, M. D.; Wolf, P.; Beck-Sickinger, A. G.; Bultmann, S.; Seitz, O. Live Cell PNA Labelling Enables Erasable Fluorescence Imaging of Membrane Proteins. *Nature Chemistry* **2021**, *13* (1), 15–23. <https://doi.org/10.1038/s41557-020-00584-z>.
- (42) Lu, Z.; Liu, Y.; Deng, Y.; Jia, B.; Ding, X.; Zheng, P.; Li, Z. OaAEP1-Mediated PNA-Protein Conjugation Enables Erasable Imaging of Membrane Proteins. *Chem. Commun.* **2022**, *58* (60), 8448–8451. <https://doi.org/10.1039/D2CC02153F>.
- (43) Scott, F. Y.; Heyde, K. C.; Rice, M. K.; Ruder, W. C. Engineering a Living Biomaterial via Bacterial Surface Capture of Environmental Molecules. *Synthetic Biology* **2018**, *3* (1). <https://doi.org/10.1093/synbio/ysy017>.
- (44) Stöhr, K.; Siegberg, D.; Ehrhard, T.; Lymperopoulos, K.; Öz, S.; Schulmeister, S.; Pfeifer, A. C.; Bachmann, J.; Klingmüller, U.; Sourjik, V.; Hertel, D.-P. Quenched Substrates for Live-Cell Labeling of SNAP-Tagged Fusion Proteins with Improved Fluorescent Background. *Anal. Chem.* **2010**, *82* (19), 8186–8193. <https://doi.org/10.1021/ac101521y>.
- (45) Csibra, E.; Renders, M.; Pinheiro, V. B. Bacterial Cell Display as a Robust and Versatile Platform for Engineering Low-Affinity Ligands and Enzymes. *Chembiochem* **2020**, *21* (19), 2844–2853. <https://doi.org/10.1002/cbic.202000203>.

- (46) Schindelin, J.; Arganda-Carreras, I.; Frise, E.; Kaynig, V.; Longair, M.; Pietzsch, T.; Preibisch, S.; Rueden, C.; Saalfeld, S.; Schmid, B.; Tinevez, J.-Y.; White, D. J.; Hartenstein, V.; Eliceiri, K.; Tomancak, P.; Cardona, A. Fiji: An Open-Source Platform for Biological-Image Analysis. *Nat Methods* **2012**, *9* (7), 676–682. <https://doi.org/10.1038/nmeth.2019>.
- (47) Zhao, B.; Tian, Q.; Bagheri, Y.; You, M. Lipid–Oligonucleotide Conjugates for Simple and Efficient Cell Membrane Engineering and Bioanalysis. *Current Opinion in Biomedical Engineering* **2020**, *13*. <https://doi.org/10.1016/j.cobme.2019.12.006>.
- (48) Zadeh, J. N.; Steenberg, C. D.; Bois, J. S.; Wolfe, B. R.; Pierce, M. B.; Khan, A. R.; Dirks, R. M.; Pierce, N. A. NUPACK: Analysis and Design of Nucleic Acid Systems. *J. Comput. Chem.* **2011**, *32* (1), 170–173. <https://doi.org/10.1002/jcc.21596>.
- (49) Schulte, M. F.; Tozakidis, I. E. P.; Jose, J. Autotransporter-Based Surface Display of Hemicellulases on *Pseudomonas Putida* : Whole-Cell Biocatalysts for the Degradation of Biomass. *ChemCatChem* **2017**, *9* (20), 3955–3964. <https://doi.org/10.1002/cctc.201700577>.
- (50) Sichert, S.; Tozakidis, I. E. P.; Teese, M.; Jose, J. Maximized Autotransporter-Mediated Expression (MATE) for Surface Display and Secretion of Recombinant Proteins in *Escherichia Coli*. *Food Technology and Biotechnology* **2015**, *53* (3). <https://doi.org/10.17113/ftb.53.03.15.3802>.
- (51) Tozakidis, I. E. P.; Lüken, L. M.; Üffing, A.; Meyers, A.; Jose, J. Improving the Autotransporter- based Surface Display of Enzymes in *Pseudomonas Putida* KT2440. *Microb. Biotechnol.* **2020**, *13* (1), 176–184. <https://doi.org/10.1111/1751-7915.13419>.
- (52) Wells, T. J.; Sherlock, O.; Rivas, L.; Mahajan, A.; Beatson, S. A.; Torpdahl, M.; Webb, R. I.; Allsopp, L. P.; Gobijs, K. S.; Gally, D. L.; Schembri, M. A. EhaA Is a Novel Autotransporter Protein of Enterohemorrhagic *Escherichia Coli* O157:H7 That Contributes to Adhesion and Biofilm Formation. *Environ Microbiol* **2008**, *10* (3), 589–604. <https://doi.org/10.1111/j.1462-2920.2007.01479.x>.
- (53) Salema, V.; Marín, E.; Martínez-Arteaga, R.; Ruano-Gallego, D.; Fraile, S.; Margolles, Y.; Teira, X.; Gutierrez, C.; Bodelón, G.; Fernández, L. Á. Selection of Single Domain Antibodies from Immune Libraries Displayed on the Surface of *E. Coli* Cells with Two β -Domains of Opposite Topologies. *PLoS ONE* **2013**, *8* (9), e75126. <https://doi.org/10.1371/journal.pone.0075126>.
- (54) Tozakidis, I. E. P.; Sichert, S.; Jose, J. Going beyond *E. Coli*: Autotransporter Based Surface Display on Alternative Host Organisms. *New Biotechnology* **2015**, *32* (6), 644–650. <https://doi.org/10.1016/j.nbt.2014.12.008>.
- (55) Keppler, A.; Gendreizig, S.; Gronemeyer, T.; Pick, H.; Vogel, H.; Johnsson, K. A General Method for the Covalent Labeling of Fusion Proteins with Small Molecules in Vivo. *Nature Biotechnology* **2003**, *21* (1), 86–89. <https://doi.org/10.1038/nbt765>.
- (56) Merlo, R.; Del Prete, S.; Valenti, A.; Mattossovich, R.; Carginale, V.; Supuran, C. T.; Capasso, C.; Perugini, G. An AGT-Based *Protein-Tag* System for the Labelling and Surface Immobilization of Enzymes on *E. Coli* Outer Membrane. *Journal of Enzyme Inhibition and Medicinal Chemistry* **2019**, *34* (1), 490–499. <https://doi.org/10.1080/14756366.2018.1559161>.
- (57) Keppler, A.; Pick, H.; Arrivoli, C.; Vogel, H.; Johnsson, K. Labeling of Fusion Proteins with Synthetic Fluorophores in Live Cells. *Proc. Natl. Acad. Sci. U.S.A.* **2004**, *101* (27), 9955–9959. <https://doi.org/10.1073/pnas.0401923101>.
- (58) Kelley, S. O.; Barton, J. K. Electron Transfer Between Bases in Double Helical DNA. *Science* **1999**, *283* (5400), 375–381. <https://doi.org/10.1126/science.283.5400.375>.
- (59) Wagner, S.; Baars, L.; Ytterberg, A. J.; Klussmeier, A.; Wagner, C. S.; Nord, O.; Nygren, P.-Å.; van Wijk, K. J.; de Gier, J.-W. Consequences of Membrane Protein Overexpression in *Escherichia Coli*. *Molecular & Cellular Proteomics* **2007**, *6* (9), 1527–1550. <https://doi.org/10.1074/mcp.M600431-MCP200>.
- (60) Verhoeven, G. S.; Alexeeva, S.; Dogterom, M.; den Blaauwen, T. Differential

- Bacterial Surface Display of Peptides by the Transmembrane Domain of OmpA. *PLoS ONE* **2009**, *4* (8). <https://doi.org/10.1371/journal.pone.0006739>.
- (61) Shi, L.; Günther, S.; Hübschmann, T.; Wick, L. Y.; Harms, H.; Müller, S. Limits of Propidium Iodide as a Cell Viability Indicator for Environmental Bacteria. *Cytometry* **2007**, *71A* (8), 592–598. <https://doi.org/10.1002/cyto.a.20402>.
- (62) Correa, I.; Baker, B.; Zhang, A.; Sun, L.; Provost, C.; Lukinavičius, G.; Reymond, L.; Johnsson, K.; Xu, M.-Q. Substrates for Improved Live-Cell Fluorescence Labeling of SNAP-Tag. *CPD* **2013**, *19* (30), 5414–5420. <https://doi.org/10.2174/1381612811319300011>.
- (63) Bucevičius, J.; Keller-Findeisen, J.; Gilat, T.; Hell, S. W.; Lukinavičius, G. Rhodamine-Hoechst Positional Isomers for Highly Efficient Staining of Heterochromatin. *Chemical Science* **2019**, *10* (7). <https://doi.org/10.1039/c8sc05082a>.
- (64) Lescrinier, E.; Esnouf, R.; Schraml, J.; Busson, R.; Heus, H.; Hilbers, C.; Herdewijn, P. Solution Structure of a HNA–RNA Hybrid. *Chemistry & Biology* **2000**, *7* (9), 719–731. [https://doi.org/10.1016/S1074-5521\(00\)00017-X](https://doi.org/10.1016/S1074-5521(00)00017-X).
- (65) Stengel, G.; Zahn, R.; Höök, F. DNA-Induced Programmable Fusion of Phospholipid Vesicles. *J. Am. Chem. Soc.* **2007**, *129* (31), 9584–9585. <https://doi.org/10.1021/ja073200k>.
- (66) Chan, Y.-H. M.; van Lengerich, B.; Boxer, S. G. Effects of Linker Sequences on Vesicle Fusion Mediated by Lipid-Anchored DNA Oligonucleotides. *Proc. Natl. Acad. Sci. U.S.A.* **2009**, *106* (4), 979–984. <https://doi.org/10.1073/pnas.0812356106>.
- (67) Shaw, A.; Lundin, V.; Petrova, E.; Fördös, F.; Benson, E.; Al-Amin, A.; Herland, A.; Blokzijl, A.; Högberg, B.; Teixeira, A. I. Spatial Control of Membrane Receptor Function Using Ligand Nanocalipers. *Nat Methods* **2014**, *11* (8), 841–846. <https://doi.org/10.1038/nmeth.3025>.
- (68) Qiu, H.; Li, F.; Du, Y.; Li, R.; Hyun, J. Y.; Lee, S. Y.; Choi, J. H. Programmable Aggregation of Artificial Cells with DNA Signals. *ACS Synthetic Biology* **2021**, *10* (6), 1268–1276. <https://doi.org/10.1021/acssynbio.0c00550>.
- (69) Wang, J.; Verbeure, B.; Luyten, I.; Lescrinier, E.; Froeyen, M.; Hendrix, C.; Rosemeyer, H.; Seela, F.; Van Aerschot, A.; Herdewijn, P. Cyclohexene Nucleic Acids (CeNA): Serum Stable Oligonucleotides That Activate RNase H and Increase Duplex Stability with Complementary RNA. *J. Am. Chem. Soc.* **2000**, *122* (36), 8595–8602. <https://doi.org/10.1021/ja000018+>.
- (70) Pitsch, S.; Wendeborn, S.; Jaun, B.; Eschenmoser, A. Why Pentose- and Not Hexose- Nucleic Acids??. Part VII. Pyranosyl- RNA (‘P- RNA’). Preliminary Communication. *Helvetica Chimica Acta* **1993**, *76* (6). <https://doi.org/10.1002/hlca.19930760602>.
- (71) Liu, C.; Cozens, C.; Jaziri, F.; Rozenski, J.; Maréchal, A.; Dumbre, S.; Pezo, V.; Marlière, P.; Pinheiro, V. B.; Groaz, E.; Herdewijn, P. Phosphonomethyl Oligonucleotides as Backbone-Modified Artificial Genetic Polymers. *Journal of the American Chemical Society* **2018**, *140* (21). <https://doi.org/10.1021/jacs.8b03447>.
- (72) Perez, A. C.; Pang, B.; King, L. B.; Tan, L.; Murrah, K. A.; Reimche, J. L.; Wren, J. T.; Richardson, S. H.; Ghandi, U.; Swords, W. E. Residence of *Streptococcus Pneumoniae* and *Moraxella Catarrhalis* within Polymicrobial Biofilm Promotes Antibiotic Resistance and Bacterial Persistence *in Vivo*. *Pathogens Disease* **2014**, *70* (3), 280–288. <https://doi.org/10.1111/2049-632X.12129>.
- (73) Du, R.; Yan, J.; Li, S.; Zhang, L.; Zhang, S.; Li, J.; Zhao, G.; Qi, P. Cellulosic Ethanol Production by Natural Bacterial Consortia Is Enhanced by *Pseudoxanthomonas Taiwanensis*. *Biotechnol Biofuels* **2015**, *8* (1), 10. <https://doi.org/10.1186/s13068-014-0186-7>.